DENTAL DOSE AND IMAGE QUALITY SURVEYS USING OPTICALLY STIMULATED LUMINESCENCE

A Thesis

by

STEPHEN MICHAEL HANDLEY

Submitted to the Office of Graduate Studies of
Texas A&M University
in partial fulfillment of the requirements for the degree of

MASTER OF SCIENCE

December 2005

Major Subject: Health Physics

DENTAL DOSE AND IMAGE QUALITY SURVEYS USING OPTICALLY STIMULATED LUMINESCENCE

A Thesis

by

STEPHEN MICHAEL HANDLEY

Submitted to the Office of Graduate Studies of
Texas A&M University
in partial fulfillment of the requirements for the degree of

MASTER OF SCIENCE

Approved by:

Chair of Committee,	Ian Hamilton
Committee Members,	John W. Poston, Sr.
	Michael Walker
Head of Department,	William Burchill

December 2005

Major Subject: Health Physics

ABSTRACT

Dental Dose and Image Quality Surveys Using Optically Stimulated Luminescence.

(December 2005)

Stephen Michael Handley, B.S., University of Missouri-Rolla

Chair of Advisory Committee: Dr. Ian S. Hamilton

The correlation of x-ray beam quality at typical energies used for dental radiography with dosimeter response was studied. Landauer Luxel ™ Optically Stimulated Luminescence (OSL) dosimeters were analyzed for the dose response with respect to the built-in variety of filters in each badge. Trends found in dosimeter response were compared to beam quality measurements through use of a spherical, air ionization chamber and added aluminum filtration to harden the beam. Additionally, a series of image quality analyses were performed to determine if the exposures were performed at optimal settings for easy reading by the dentist. Through the use of a survey in which the dental office sends in the x-ray film to Landauer for analysis, these factors can be determined using calibration curves determined from collected data for correction.

ACKNOWLEDGMENTS

I would like to thank my committee chair, Dr. Hamilton, my committee members, Dr. W. Poston, Sr., and Dr. Walker, for their time and support throughout the writing of this paper. I would also like to thank Dr. Joel Gray, Mark Salasky, Dr. Brian Markey, and Ryan Ford for their insight and guidance pertaining to this research during my internship at Landauer.

TABLE OF CONTENTS

Page

ABSTRACT..... iii

ACKNOWLEDGMENTS..... iv

TABLE OF CONTENTS..... v

LIST OF FIGURES..... vii

LIST OF TABLES..... ix

INTRODUCTION..... 1

BACKGROUND..... 3

- X-RAY MACHINE OPERATION..... 3
- PHOTON INTERACTIONS, BEAM CHARACTERIZATION..... 5
- ION CHAMBER OPERATION..... 10
- OPTICALLY STIMULATED LUMINESCENCE..... 12
- RADIOGRAPHIC FILM..... 15
- PREVIOUS WORK AND PRESENT STATUS OF PROBLEM..... 16

MATERIALS AND METHODS..... 20

RESULTS..... 30

DISCUSSION..... 39

SUMMARY AND CONCLUSIONS..... 42

Page

REFERENCES..... 44

APPENDIX A..... 46

APPENDIX B..... 48

APPENDIX C..... 50

APPENDIX D..... 51

VITA..... 52

LIST OF FIGURES

FIGURE		Page
1	The inner workings of a typical x-ray machine	4
2	Typical dental x-ray machine	5
3	X-ray spectra showing bremsstrahlung, characteristic x-rays, and the effects of filtration	8
4	Typical cylindrical ion chamber probe geometry	11
5	OSL electron and hole traps	13
6	Landauer Luxel dosimetry badges	14
7	The filter positions within a Luxel dosimetry badge	14
8	Phillips MG320 x-ray generator with cone attached	21
9	Plastic dosimeter holder and ion probe positioning	22
10	Box cart, dosimeter holder, and x-ray machine – view 1	23
11	Box cart, dosimeter holder, and x-ray machine – view 2	24
12	Keithley 35040 electrometer	25
13	X-ray machine control box	26
14	HVL vs. OW/Sn ratio	32

FIGURE Page

15 Optical densities: D speed film..... 33

16 Optical densities: F speed film..... 33

17 Representative pictures of digitalized film..... 34

18 Labview analysis of film relative optical density: Cu and Sn filters..... 35

19 Labview analysis of Cu mesh..... 36

20 Labview reported pixel values calibration..... 37

21 Cu mesh image quality analysis..... 38

LIST OF TABLES

TABLE		Page
1	Minimum HVLs for dental x-ray machines	9
2	K-shell x-ray fluorescence energies in tungsten	10
3	Intraoral film-speed classification	15
4	Change in filter thickness with tube voltage	26
5	Ion chamber air kerma rates	30
6	Sample HVL calculation - 50 kVp, 1.8 mm inherent filtration	31

INTRODUCTION

The need exists for a quick, inexpensive, and reliable way for dental facilities to test both the output of their x-ray equipment and the quality of their film processing to ensure the most accurate results. Most states mandate by law the testing of x-ray equipment on a periodic basis. Often, this means having a certified physicist or state inspector arrive on site to complete a series of tests to verify that x-ray equipment is operating in accord with the proper criteria. This technique is time consuming, and because of the low dose and low risk that dental equipment poses to operators and patients, many dental facilities fall behind on testing.

One objective of this research was to provide a method through which the quality of the x-ray beam could be remotely analyzed. Different dental facilities and x-ray machines can be quickly tested and the results reported through use of a mail-in dental dose survey. The dose and half-value layer (HVL) would be reported after being analyzed at Landauer. Luxel + Optically Stimulated Luminescence (OSL) badges are to be read by the aforementioned company to acquire the needed data. Facilities that show deviation outside the accepted norm can be flagged for a more intensive follow-up visit by state inspectors.

Another objective of this research was to provide a method through which the quality of the film processing at the dental facility could be analyzed. Many different aspects can affect the quality of film processing including developing temperature,

---

This thesis follows the style of Health Physics.

developing time, developer and fixer purity, and darkroom cleanliness and quality control. Each of these factors introduces variability and thus reduces both the accuracy and precision of the final image that can be analyzed. Included in the proposed mail-in survey would be a test to determine if the film is being processed properly.

BACKGROUND

There are several important concepts with which the reader should be familiar to understand the research presented in this paper. These concepts include how x-rays are generated, photon interactions and characterization, ion chamber operation, OSL dosimeter technology, and the use of radiographic film. After these concepts are explained, previous work related to this research will be discussed.

X-RAY MACHINE OPERATION

X-ray machines consist of several components: a cathode, an anode, a cooling mechanism for the assembly, shielding, and a window for the x-rays to exit the assembly. Figure 1 depicts a typical x-ray machine setup. X-rays are produced when electrons originating from the cathode, a metal filament, interact with the anode. A current is applied to a heater on the cathode to produce this source of free electrons. A high potential difference serves to accelerate the electrons from the cathode to the anode. Additionally, a vacuum is utilized to increase the mean free path of the electrons, thereby maximizing the collection efficiency of the electrons at the anode. The anode, or target, is typically made of tungsten and during operation can get very hot because of the enormous amount of kinetic energy imparted by the incoming electrons. Circulating water or cooling oil is typically used to help decrease the operating temperature of the anode.

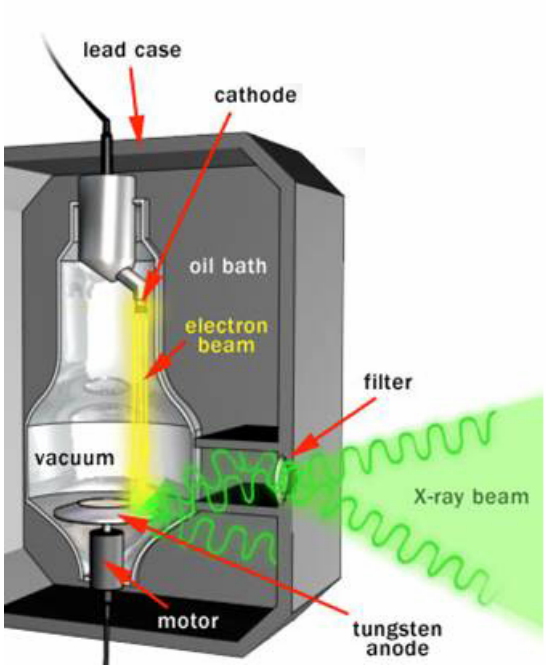

Figure 1: The inner workings of a typical x-ray machine (Harris 2002)

Electrons can interact with the target in several different ways. The first way is through characteristic x-ray emission. Here, accelerated electrons impart energy to higher binding-energy electrons in target atoms. If the incoming electron has enough energy to overcome the binding energy of the electron shell, the shell electron is released from its orbit. Immediately following this, an electron from a higher (lesser bound) shell drops down to fill the vacancy just created. In the process, a monoenergetic, characteristic x-ray is produced.

The second method in which photons are produced is through bremsstrahlung. In this process, free electrons travel close to the nucleus of a target atom and the close proximity to the nucleus causes the electrons to alter their trajectory. This momentum change in the trajectory of the free electron causes it to slow down and release a

spectrum of photon energies. Characteristic x-rays are emitted isotropically, but the photons generated as bremsstrahlung have a directional dependence based on the energy of the incoming electron. Both sources of photons are collimated through use of dense shielding around the x-ray tube assembly. Figure 2 shows a typical dental x-ray machine and the tube assembly for beam collimation.

Figure 2: Typical dental x-ray machine (Animal Clinic 2005)

PHOTON INTERACTIONS, BEAM CHARACTERIZATION

There are three basic ways photons interact with matter to transfer appreciable amounts of energy: photoelectric absorption, Compton scattering, and pair production. In photoelectric absorption, a free electron is produced with energy equal to the difference between the incident photon energy and the binding energy of shell where the

photon-bound electron interaction occurred. In Compton scattering, an incident photon interacts with an electron transferring some of its energy to the electron in the process. Maximum energy is transferred to the recoil electron when the secondary photon is scattered at an angle of 180° from the trajectory of the incident photon. In pair production, the photon is converted into a photon and an electron. The energy of the incident photon is shared between the two particles produced. Each of these three interactions is dominant at specific photon energies in relation to the target material atomic number. Photoelectric absorption and pair production are highly dependent on the atomic number, Z, of the material. Compton scattering is dependent on the Z of the absorber to a much lesser degree than photoelectric absorption or pair production. Pair production is not a concern in dealing with x-ray machines because the photon energy is much less than the 1.02 MeV needed to become energetically possible.

Photons can be attenuated through the use of shielding material such as aluminum, copper, or lead. Attenuation increases as a strong function of Z in the filtering material because the higher interaction coefficient of photoelectric absorption at higher values of Z. Thus, it takes a smaller thickness of lead to attenuate the same amount of photons as a material of a lower Z material such as aluminum. The equation relating the initial intensity and the final intensity after attenuation is:

$$I = I_0 e^{-\mu x} \quad \textbf{(1)}$$

where I_o is the initial intensity, μ is the linear attenuation coefficient and x is the thickness of the material.

A typical x-ray beam can be described either in terms of its energy spectrum or its attenuation characteristics in a reference medium. The use of HVL is an accepted standard in which the mean characteristics, or "quality" of the x-ray beam can be described in relation to how the beam is attenuated through a specified material, such as aluminum. The HVL is calculated by finding the thickness of the filtration material required to reduce the intensity to one-half the original value.

Once the HVL thickness is known, the mass attenuation coefficient is calculated by utilizing this thickness and the density of the filtering material. The average beam energy can then be determined through use of established tables relating the mass attenuation coefficient to the average beam energy.

Beam characteristics can vary a great deal from one x-ray machine to another. Each x-ray generator typically operates at a set kilovolt peak (kVp) for a given diagnostic procedure. The National Council of Radiation Protection and Measurements (NCRP) recommends that the operating potential be between 60 and 80 kVp for dental exposures (NCRP 2003). The operating potential of the x-ray machine determines the maximum energy of the bremsstrahlung spectrum.

A completely unfiltered bremsstrahlung spectrum would have an energy spectrum similar to line 'A' in Figure 3. Added filtration attenuates photons of all energies but its reduction of lower energy photons is more pronounced. Lines 'B', 'C', and 'D' in Figure 3 show the effects of additional filtration on the spectrum with 'D' incorporating the most filtration.

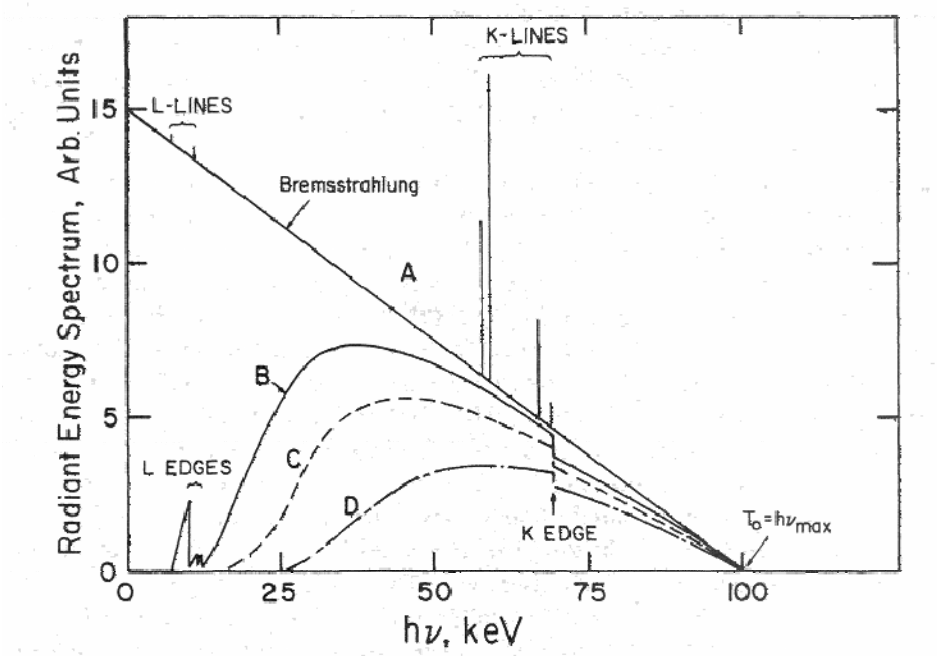

Figure 3: X-ray spectra showing bremsstrahlung, characteristic x-rays, and the effects of filtration (Attix 1986)

The Food and Drug Administration recommends that dental x-ray machines incorporate enough inherent filtration to achieve a minimum HVL as displayed in Table 1. Most states, including Texas, have incorporated these recommendations in their own regulations (TDSHS 2004). The amount of inherent filtration varies from one x-ray machine model to another but many manufacturers incorporate roughly 2.5 mm of aluminum to harden the beam as required.

Table 1: Minimum HVLs for dental x-ray machines (FDA 1997)

Designed operating Range (kVp)	Measured operating potential (kVp)	HVL (mm Al)
Below 50……	30	0.3
	40	0.4
	49	0.5
50 to 70……..	50	1.2
	60	1.3
	70	1.5
Above 70……..	71	2.1
	80	2.3
	90	2.5
	100	2.7
	110	3
	120	3.2
	130	3.5
	140	3.8
	150	4.1

Also shown in Figure 3 are several monoenergetic, characteristic x-ray peaks. The most prominent of these peaks, shown at 55 keV, is the result of a K-shell vacancy (in tungsten) being filled by an electron from an outer (lesser bound) orbit. A 55 keV fluorescence photon is released during completion of this orbital transition. The K-shell x-ray fluorescence energies vary depending on the target used. The most common x-ray tube target is tungsten and its fluorescence energies and yields are tabulated in Table 2.

Table 2: K-shell x-ray fluorescence energies in tungsten (Attix 1986)

Transition	Designation	Energy (keV)			Relative No. of Photons	
K–L_{III}	α_1	59.321			100	
K–L_{II}	α_2	57.984			57.6	
K–M_{II}	β_3	66.950			10.8	
K–M_{III}	β_1	67.244	$\cong$ 67.2		20.8	32.1
K–M_{IV}	$\beta_{5/1}$	67.654			0.233	
K–M_V	$\beta_{5/2}$	67.716			0.293	
K–N_{II}	$\beta_{2/1}$	69.033			2.45	
K–N_{III}	$\beta_{2/2}$	69.101			4.77	
K–N_{IV}	$\beta_{4/1}$	69.269	69.276	$\cong$69.1	0.127	8.4
K–N_V	$\beta_{4/2}$	69.283				
K–O_{II}	$\beta_{2/3}$	69.478	69.484		1.07	
K–O_{III}	$\beta_{2/4}$	69.489				

ION CHAMBER OPERATION

Ionization chambers consist of two electrodes separated some distance in a gas enclosure across which is applied a potential difference (Figure 4). There are many different fill gases available, but the most common are noble gases, air, and methane. Photons interact within the gas volume and the cathode wall, ultimately creating ion pairs. The electrons are attracted to the anode and the slower moving, positively charged ions to the cathode. A potential difference is applied to aid in charge migration. If it were not for this, recombination would be the most likely event.

There are several different applied voltage regions of operation used with gas filled detectors: ion saturation, proportional region, and the Geiger-Mueller region. Ion chambers apply just enough voltage to stay in the ion saturation region. The chamber is operated in this region to prevent recombination of the ion pairs so that the ion pairs have a chance to migrate to the anode and cathodes. When the ion pairs reach the anode

and cathodes, a net charge is built up and this charge is proportional to the ionization caused by the incident radiation.

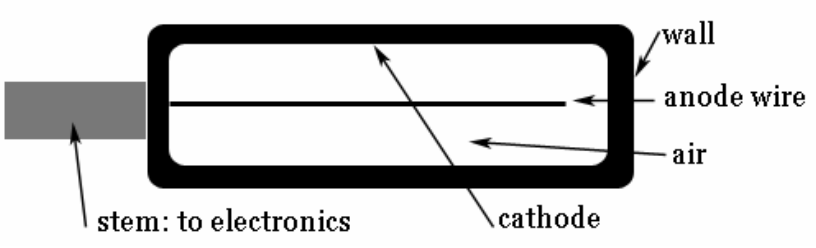

Figure 4: Typical cylindrical ion chamber probe geometry

The absorbed dose can be determined from the ionization produced within the ion chamber by the use of the Bragg-Gray theory (Martin 2000). The relationship between the ionization produced in the gas and the dose is as follows:

$$D_{gas} = \frac{Q}{m_{gas}} W \tag{2}$$

where Q is the charge collected, and m_{gas} is the mass of the detector fill gas. The W value is specific to the fill gas utilized and is expressed in units of eV per ion pair. For the Bragg-Gray theory to be valid, the chamber walls should be thick enough so that secondary electrons will be stopped within the walls. Additionally, the gas volume dimensions should be small so that its presence does not perturb the charged particle field (Attix 1986). With these two conditions met, Equation 2 can be used to relate the absorbed dose in a probe inserted into a medium to that in the medium itself (Attix 1986).

OPTICALLY STIMULATED LUMINESCENCE

OSL dosimeters are similar to thermoluminescent dosimeters (TLDs). Like TLDs, OSL dosimeters store energy imparted by radiation quanta through use of electron and hole traps. Photons can interact with the OSL material (commonly aluminum oxide, Al_2O_3, doped with small amounts of carbon) causing electrons or holes to migrate between the conduction and valence bands. Figure 5 illustrates the inclusion of trap sites between the conduction and valence bands. A photon may impart its energy, elevating an electron to an excited state. This electron has enough energy to bridge the gap from the valence to the conduction band. Eventually, the electron will return to a lower (more bound) energy level and falls from the conduction band. Sometimes this electron will fall into a trap before it reaches the valence band. In this case, the trap will effectively store the energy of this elevated level by stopping the electron until enough light at the appropriate wavelength is applied to the Al_2O_3 to release the electron. The wavelength of light used for excitation is different from that of the emitted photon. The intensity of the light from the emitted photons is directly proportional to the energy imparted to the OSL material by the initial, incident radiation.

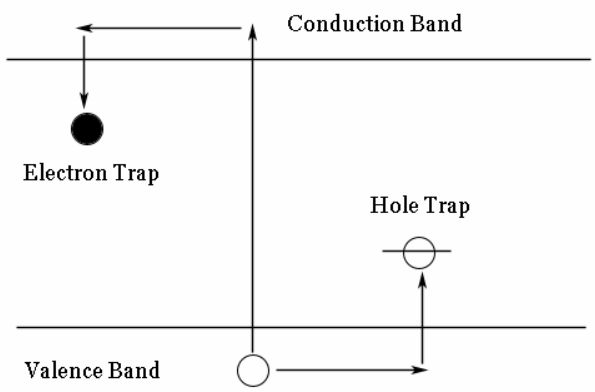

Figure 5: OSL electron and hole traps

The Luxel OSL dosimetry badge consists of the following components: doped Al_2O_3 material, a copper filter, a tin filter, a plastic filter, cutout for an open-window, a protective plastic housing, a copper grid, and labeling for identification purposes. The aluminum oxide material is positioned uniformly behind the different filters. These filters provide varying amounts of attenuation; tin (Sn) provides the most attenuation, followed by copper (Cu), plastic (Pl), and the open-window (OW). The open-window consists of a very thin layer of plastic, which provides negligible radiation attenuation. Figure 6 shows several Luxel dosimetry badges – notice the small hole for the open-window. Figure 7 shows the positions of the filters within the badge.

Figure 6: Landauer Luxel dosimetry badges

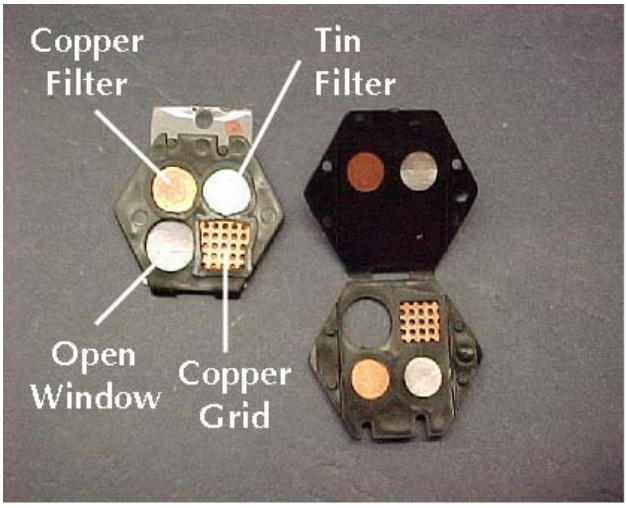

Figure 7: The filter positions within a Luxel dosimetry badge

A copper grid is also included in the Luxel badge. This grid is normally used to help determine if the dose received was from a static or dynamic (moving) exposure. In this experiment, the grid will be used to provide information regarding image sharpness such as focal spot blur.

RADIOGRAPHIC FILM

Dentists have a variety of choices when selecting an image receptor system. Today, there are two broad categories of image receptor systems: intraoral film and direct digital radiography. Each system has its advantages but because of the high initial cost of a direct digital radiography system, most dental offices still rely on radiographic film.

Recent advances in radiographic film technology have decreased the exposure level needed to achieve desired contrast on developed x-ray film. Patient exposure can be decreased by a factor of two by moving to a sequentially higher film-speed group. Today, there are four main types of film classified by their speed range in units of inverse roentgen. These categories and their respective speed range are shown in Table 3. The NCRP currently recommends that film-speeds E and greater be used in dental practice; however, many offices still use D speed film (NCRP 2003). In this experiment, tests will be performed both on D and F speed film.

Table 3: Intraoral film-speed classification (NCRP 2003)

Film-Speed Group	Speed Range (R^{-1})
C	6-12
D	12-24
E	24-48
F	48-96

PREVIOUS WORK AND PRESENT STATUS OF PROBLEM

The National Council on Radiation Protection and Measurement (NCRP) published the following recommendations concerning dental x-ray machine inspections: (NCRP 2003)

> All new dental x-ray installations and existing installations not previously surveyed shall have a radiation protection survey performed by, or under the direction of, a qualified expert. Resurveys shall be performed at regular intervals thereafter. The resurvey interval should not exceed 4 y. In addition, a resurvey shall be made after any change in the installation, workload, or operating conditions that might significantly increase occupational or public exposure (including x-ray machine service or repair that could affect the x-ray machine output or performance.)

Many on-site surveys have been conducted by physicists to ensure that x-ray equipment performance satisfies the recommendations set by the NCRP (NCRP 2003). Parameters such as x-ray generator waveform, kVp, milliampere, and timer range, the amount of inherent filtration, Half-Value Layer (HVL), and the x-ray tube head leakage can be tested and verified on site. TLDs have been used in the past to monitor the dose at various locations with respect to the x-ray tube target. Research outlined herein combined laboratory beam quality measurements using an ionization chamber with data obtained through the use of OSL dosimeters. Data from the dosimeters were used to determine both the dental entrance dose and x-ray beam quality.

Correct operation and care of the x-ray machine provides only half the solution to an ideal x-ray exposure. The other issue to consider is dental film processing. Many

experiments have been performed in the past to determine quality control for dental film processing and development. One study evaluated over 1000 radiographs from dental offices for errors (Svenson et al. 1994). This research found that nearly 70% of respondents showed problems such as projection and film density errors. In addition, quality control of film development is important and shouldn't be ignored.

There are many parameters to consider to ensure proper film processing. These parameters include: the processing temperature, the quality of developer and fixer chemicals, the amount and type of light present in the darkroom, and the type of film used. All of these factors affect the resulting film quality. The effect of developer temperature on direct exposure film was presented by Kircos et al. (1989). This research found that minimal diagnostic compromise would result from moderate changes in temperature for D and E speed films.

Findings from a previous dental survey were presented in a paper by Kaugars et al. (1985). This survey received 2,257 replies and gathered information from dental offices nationwide a variety of parameters including: film processing, patient safety, and x-ray machine parameters such as kVp and exposure time, and technique. These findings gave a general idea of the strengths and weaknesses in many clinics nationwide. Weaknesses pointed out included: the variables of manual film processing were not well controlled at many facilities, many darkrooms had excessive light, rectangular cones are not used by many dentists, and there was minimal participation by dentists and dental hygienists in courses on radiation safety.

Napier published dose distributions for various intra-oral and panoramic x-ray sets (Napier 1999). This paper referenced results from the National Radiological Protection Board (NRPB) Dental X-ray Protection Services to develop a reference dose for intra-oral radiography and panoramic radiography.

In a study by Yakoumakis et al. (2001), aspects of dental radiographic image quality, exposure time settings, and film processing were assessed in relation to radiation dose. Their results indicated great variability in exposure time settings and deficiencies due to inadequate film processing.

Stavrianou et al. (2005) evaluated over 50 intraoral x-ray units in Greece. Parameters such as equipment maintenance, film speed, and film processing conditions were analyzed. In addition, radiologic characteristics such as tube voltage and leakage, type of collimation, timer accuracy, and entrance dose were analyzed. On site inspections, QA tests, and standard questionnaires were performed to acquire these data. This research found that film processing conditions were at many facilities deficient and in need of improvement.

Many on-site surveys have been performed in the past and many survey questionnaires have been sent out as previous research. These surveys differ from the dental survey outlined in this paper. Most of the questionnaire surveys were subjective in nature and focused on the opinion and knowledge of the dentists at the facilities surveyed. The on-site surveys shared some similarities to this research such as the measurement of beam HVLs, film processing quality determination, and use of dosimeters for dose determination. This research adds to and pulls all these aspects together to determine the quality of on-site film processing and dental dose through use of mail-in surveys utilizing OSL technology.

MATERIALS AND METHODS

The concept is to place an x-ray film on a surface and overlay it with a Luxel standard personal dosimetry badge. The badge contains three different filters: tin, copper, plastic, and an open-window. Additionally, a copper mesh pattern is included in the badge. The key component of OSL (Al_2O_3:C) is sandwiched inside the badge behind the filters. The Al_2O_3:C and the filters are held into place by a plastic holder, which makes up the outermost portion of the badge. The badge is held at a distance of 2.54 cm in front of the dental film by a cardboard overlay. This distance is utilized so that the film sharpness behind the copper grid can be objectively analyzed later.

The dose and the beam quality characteristics are determined using the following procedure. A Phillips MG320 x-ray generator was used for all subsequent exposures throughout this experiment and is shown in Figure 8.

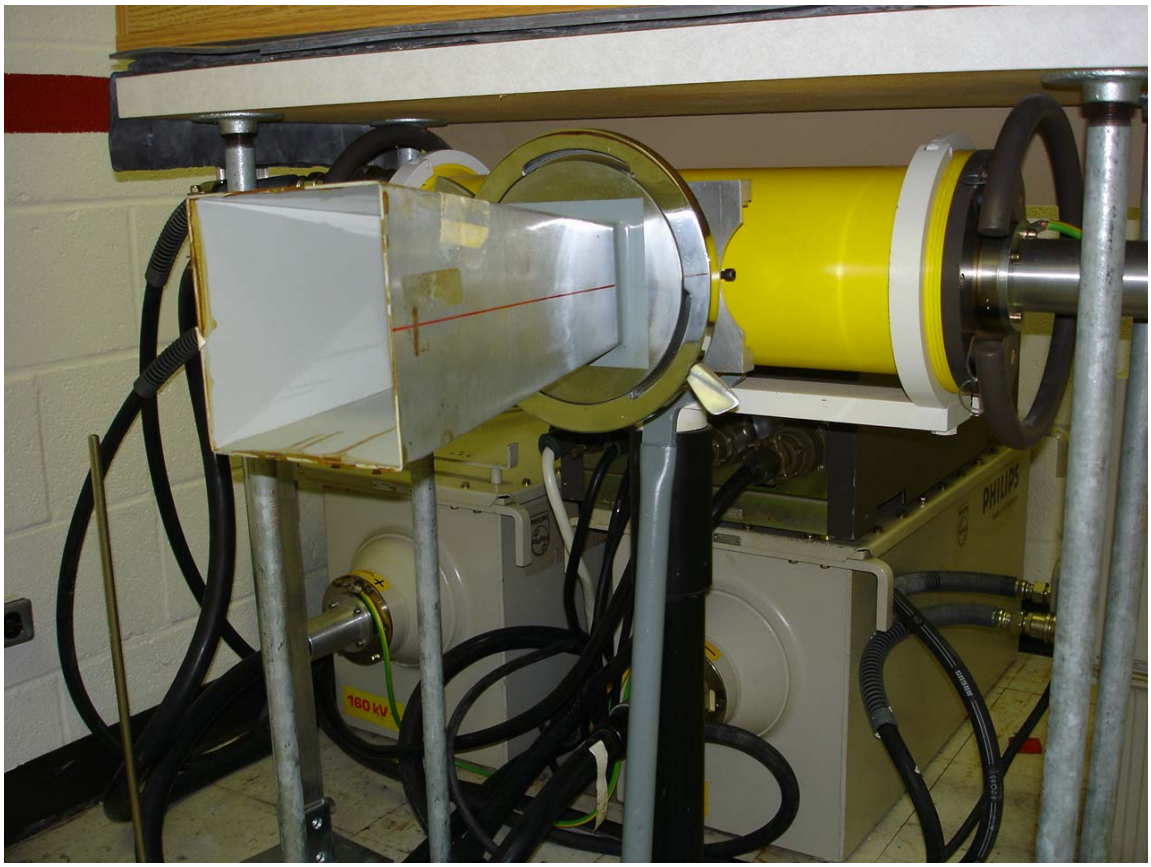

Figure 8: Phillips MG320 x-ray generator with cone attached

The x-ray beam at Landauer is directed horizontally at a height of roughly 3 ft above the floor. A medium sized (8 cm x 8 cm x 16 cm) square aluminum cone is attached to the end of the x-ray machine. A sliding track on which a box was mounted in front of the x-ray tube allows for exposures to be made at different distances. This platform is positioned at a distance of 160 cm from the end of the x-ray tube cone. A thin, 1 mm, plastic sheet is mounted vertically to the front side of the mobile box. The plastic sheet has cutouts in it so that 5 Luxel dosimeters could be snapped into the sheeting and held securely. This sheet allows the dosimeters to be vertically centered in

the x-ray beam. Figures 9, 10, and 11 show the positioning of the dosimeter holder, the ion chamber probe, and the x-ray cone.

Figure 9: Plastic dosimeter holder and ion probe positioning

Figure 10: Box cart, dosimeter holder, and x-ray machine – view 1

Figure 11: Box cart, dosimeter holder, and x-ray machine – view 2

An Exradin A3-111 air ionization chamber probe was centered vertically and horizontally in front of the dosimeter holder. The probe was attached to a Keithley model 35040 electrometer. Figure 12 shows the display of the electrometer. The electrometer had calibration factors programmed in it for different average beam energies reported during its last calibration. This ion chamber setup was utilized to determine the current needed to deliver the correct dose to the dosimeters described next in the procedure.

Figure 12: Keithley 35040 electrometer

Next, five dosimeters were loaded into the plastic holder (Figure 9) and an exposure made. A dose of 5 mGy was delivered over a time interval of 1 minute at 50 kVp with 1.8 mm of aluminum filtering added to the end of the cone. The current needed to deliver this dose was determined previously using the ion chamber readings. This procedure was then repeated for 60, 70, and 80 kVp. The added aluminum filter thickness varied with the kVp as shown in Table 4. The current was adjusted at each different operating potential to keep the total dose at 5 mGy. Figure 13 shows the control box used to set the x-ray machine operating potential, current, and exposure time.

Table 4: Change in filter thickness with tube voltage

Tube Voltage (kVp)	Added Filtration (mm Al)
50	1.8
60	2.4
70	3.0
80	2.8

Figure 13: X-ray machine control box

After the badges had been exposed, they were read and processed on-site. Counts from the OSL readers for the various filter positions were retrieved and saved to an Excel file. Data sets were collected for each beam setting.

Next, a series of HVL calculations were performed for this specific x-ray machine setup. The basic setup for this test was as described above with a medium-sized square cone attached to the x-ray machine, a horizontal distance of 160 cm between the end of the cone and the front of the mobile box, and the ionization probe attached to the front of the box. The HVL was calculated for inherent filter thicknesses of 1.8, 2.4, 2.8, and 3.0 mm Al and potentials of 50, 60, 70, 80 kVp. Additional aluminum sheets were added in front of the cone to establish the range of dose needed for the HVL calculations.

For calculating the HVL of 1.8 mm Al and 50 kVp, the following measurements were taken. First, the 1.8 mm Al filter was attached in front of the cone and the x-ray tube potential set to 50 kVp. The current was initially set so that the dose would be less than 1 mGy for a 1 minute exposure. No added filter sheets were added to the end of the cone and an exposure was made. Next, extra sheeting was added so that just less than half of the photons were attenuated. Finally, another exposure was performed so that just more than one-half of the photons were attenuated. With these data, the HVL for 1.8 mm Al and 50 kVp can be calculated through interpolation. As described above, this procedure was repeated for the rest of the filter thicknesses and operating potentials.

The film processing quality was analyzed as follows. First, the sliding box was moved to a distance of 160 cm from the end of the medium-sized cone attached to the x-ray machine. To eliminate extra variables, the thickness of aluminum filtering added to the end of the x-ray cone was kept constant. The thickness of aluminum filtering used was that which produced a HVL of 1.7 mm Al at 70 kVp. This thickness turned out to be

1.3 mm Al. Next, the acrylic holder (mentioned above) was placed on the front of the box. The cardboard holder for the x-ray film-Luxel badge was centered relative to the x-ray beam on this plastic holder. The x-ray film was taped to the inside of the cardboard holder and the Luxel badge was taped on the front of the cardboard, serving as a phantom for the x-ray film. Two different x-ray films were tested: D speed and F speed. The x-ray machine was set up utilizing potentials of 50, 60, and 70 kVp for each of the different film types. The criterion for the exposure was to produce an optical density of 0.30 when analyzed with a densitometer on the developed x-ray film for the region shielded by the tin filter. This optical density was chosen to ensure that the ideal optical density range would be utilized for the range of exposure. For 50 kVp, this corresponded to 25 mAs. All exposures were for 10 s. This criterion was defined as "1x normal exposure". In addition, "1/2x normal" and "2x normal" exposures were performed. All of the film was developed in a darkroom with the aid of an automatic film developer. Once all the film was developed and labeled, the optical densities of the three filter positions and the background were measured using a densitometer.

The next major step in analyzing film processing quality was to digitize the image and analyze it using a program written in-house at Landauer called Image Analyzer. A Nikon Coolscan 5000ED slide scanner was used to digitize the x-ray film. The film needed to be cropped lengthwise by several mm and was placed in standard 35mm slide mounts. Each of the films was scanned as a 5000 dpi 8-bit uncompressed Tag Image File Format (tiff) file. Each of the tiff files was imported and analyzed using Image Analyzer. Image Analyzer is a program built via Labview that allows the user to

extract brightness or darkness levels analyzed horizontally across the entire tiff file. These optical density levels can be imported into Excel for further analysis. Additionally, Image Analyzer can be used to compute the Fourier transform of the copper mesh pattern, giving an indication of the image sharpness.

A correlation was derived between the relative contrast levels reported by Image Analyzer and the correct values given by a densitometer. A sensitometer was used to create a step-wedge of varying optical densities. The optical densities of the wedges were read using a densitometer. Next, the step-wedge was scanned and the resulting tiff file opened in Image Analyzer. The optical densities reported by Image Analyzer were recorded for each wedge. A calibration curve was constructed relating the digitized optical density with the true optical density.

RESULTS

The x-ray machine current was varied with each kVp setting to ensure that the total dose delivered to the dosimetry badges was close to 5 mGy for each operating potential. The results from the ionization chamber showing the air kerma, the current, the kVp, and the time are shown below in Table 5.

Table 5: Ion chamber air kerma rates

Tube Voltage (kVp)	Added Filtration (mm Al)	Exposure Time (min)	Current (mA)	Average Air Kerma Rate (mGy/min)
50	1.8	0.97	4.50	5.15
60	2.4	1.03	3.65	4.85
70	3.0	0.99	3.40	5.04
80	2.8	0.86	2.90	5.79

The first HVL was determined for the x-ray beam for an operating potential of 50 kVp and 1.8 mm of inherent filtration of Al. Table 6 is provided to help explain the HVL calculation for these parameters. With no added filtration, a kerma of 1.63 mGy was recorded. Half of this initial air kerma is 0.81 mGy. To achieve data points relatively close to this value, it took 1.508 and 1.754 mm of added aluminum. Next, the logarithm of each of these air kerma values was calculated. Finally, an interpolation was performed to find the thickness needed to achieve an air kerma of 0.81 mGy.

Table 6: Sample HVL calculation - 50 kVp, 1.8 mm inherent filtration

Starting Filtration (mm Al)	Potential (kVp)	Current (mA)	
1.8	50	1.5	
Added Filtration (mm Al)	**Air Kerma (mGy)**	**LogKerma**	**Half-Value**
0	1.63	0.21	0.81
1.508	0.82	-0.09	
1.754	0.73	-0.14	
Slope	-0.19	**True HVL (mm Al)**	1.5
Intercept	0.20	**Difference**	-1%
HVL (mm Al)	1.52		

The first HVL was also determined for the operating potentials: 60, 70, and 80 kVp. The results for all kVp settings and inherent filtrations used are given in APPENDIX B.

Five Luxel dosimetry badges were exposed at each condition outlined above. The raw data from these dosimeters, including the differences due to the various filters included in these dosimeters, are given in APPENDIX A. A correlation was found between the open window to tin ratio (OW/Sn) and the first half-value layer. This is shown in Figure 14. The curve fit was derived using a power series fit to the data points. Of the four filter positions, Sn was the only position to increase in OSL reading as the first HVL was increased. The OW position was chosen in the ratio to maximize the slope as the first half-value layer increased.

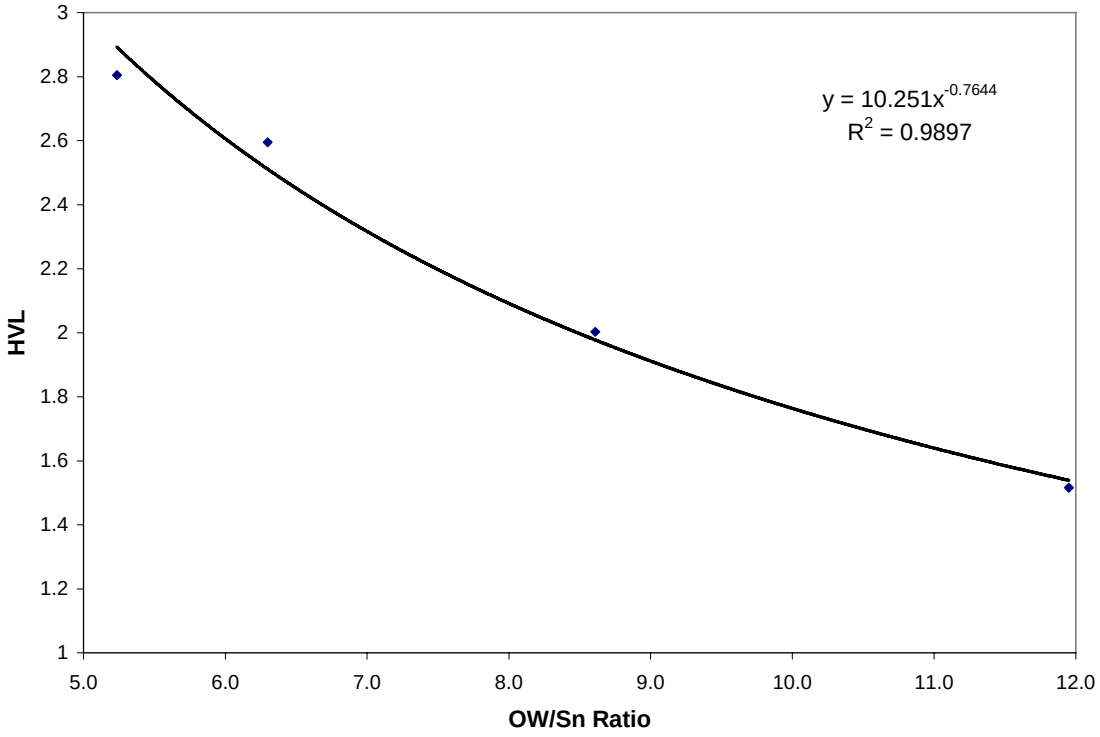

Figure 14: HVL vs. OW/Sn ratio

The exposure time and current were varied to achieve an optical density of 0.30 in the film behind the tin filter (this was defined as "normal exposure"). The required mAs was found by trial and error and is given in APPENDIX C. Once these settings were determined, the effects of double or half this exposure could be determined. The range of useful optical densities is from 0.30 to 3.00. The optical densities at different regions of the x-ray film are shown in Figures 15 and 16 for D and F speed film, respectively.

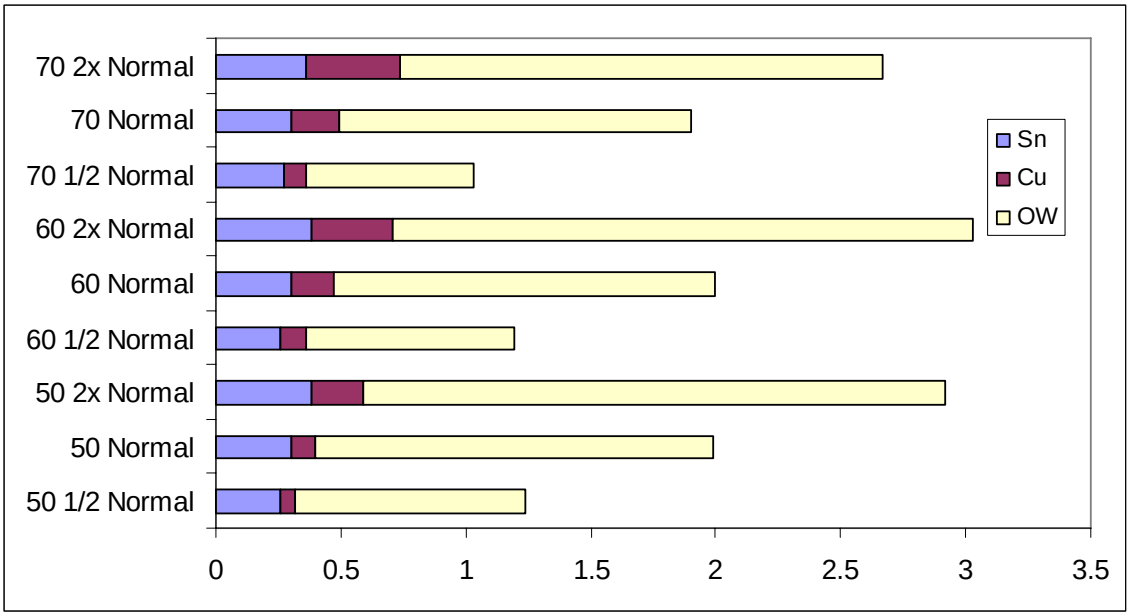

Figure 15: Optical densities: D speed film

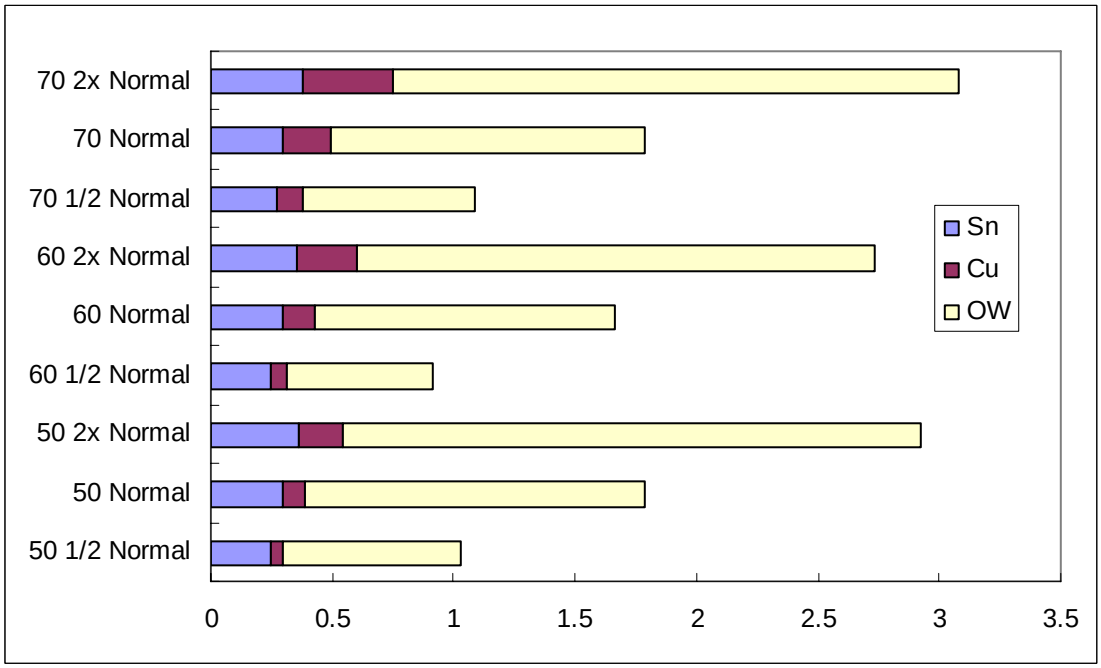

Figure 16: Optical densities: F speed film

A representative scan in the process of digitizing the film using the film scanner is shown in Figure 17.

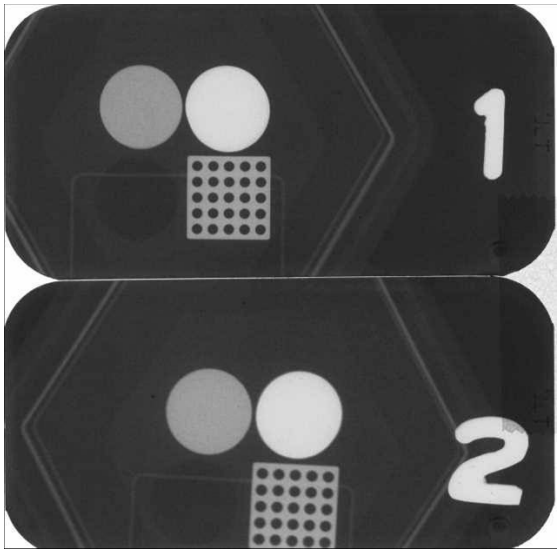

Figure 17: Representative pictures of digitized film

After importation of this film into Labview, the pixel brightness was evaluated in a straight line covering both the tin filter position (brightest circle in Figure 17) and the copper filter position (second brightest circle). Figure 18 shows the pixel brightness values across these filters. A higher pixel brightness in the y-axis of the figure corresponds to a darker optical density. The pixel brightness was also evaluated in a straight line covering both the open window position and the copper grid (specifically focusing on the grid). Figure 19 below shows the pixel brightness values across the Cu mesh.

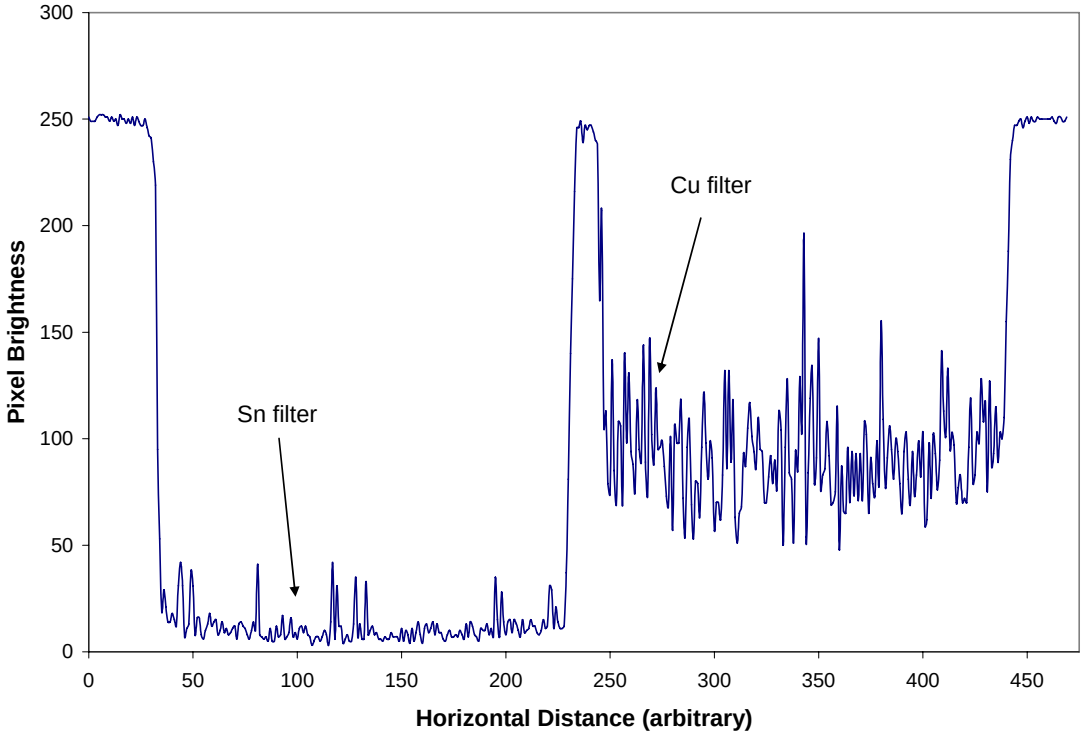

Figure 18: Labview analysis of film relative optical density: Cu and Sn filters

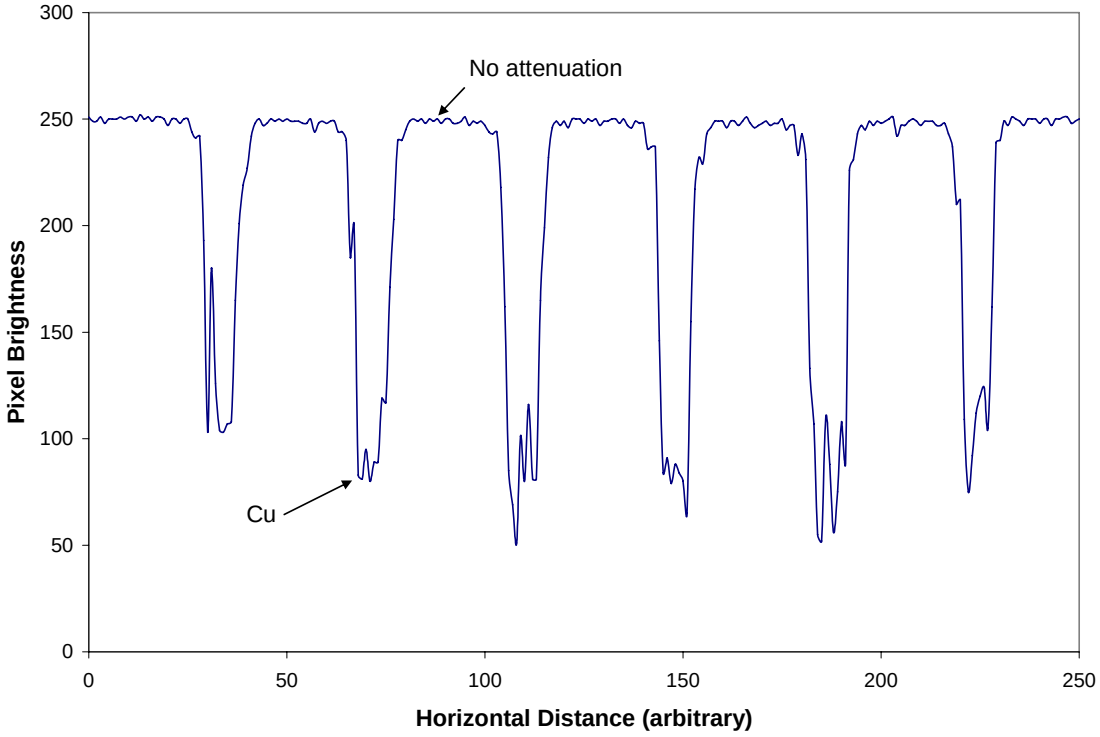

Figure 19: Labview analysis of Cu mesh

The relationship between the arbitrary pixel brightness values reported by Labview and the actual optical density is shown in Figure 20.

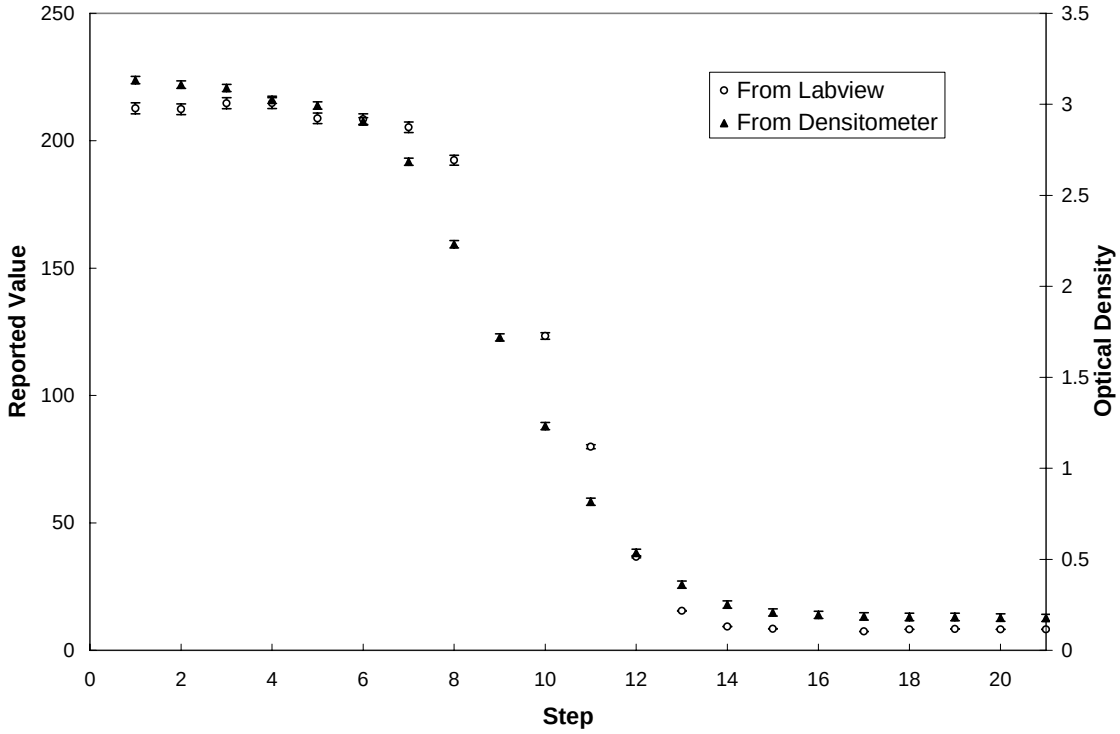

Figure 20: Labview reported pixel values calibration

Image sharpness was evaluated by focusing on the Cu mesh within the Labview program written in-house at Landauer. The Labview program can be used to perform a series of calculations utilizing Fourier transforms to assign a numerical value to the sharpness. Figure 21 shows the results comparing the sharpness of two different exposure conditions: The software reports a value of '10' as ideal and '1' as poor. Film 1 of Figure 21 was created by placing the Luxel dosimeter flush against the film within the cardboard holder during its exposure. The image is sharp and represents ideal processing conditions. Image analyzer assigned a value of 10 to this image quality. Film 2 of Figure 21 is less sharp and is simulated by increasing the distance between the dosimeter and the film to 2.54 cm during the exposure. Increasing the distance between the phantom

and the film and the phantom increased the focal spot scatter resulting in more image blur around the mesh.

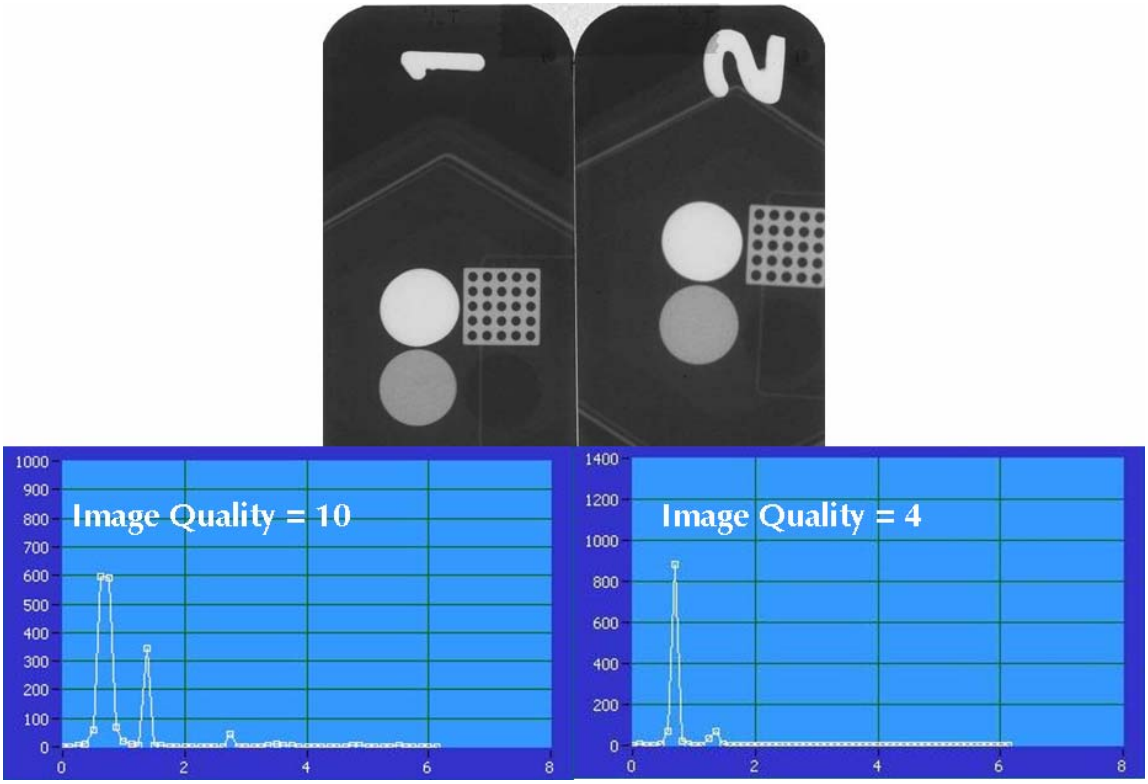

Figure 21: Cu mesh image quality analysis

DISCUSSION

Both the amount of inherent filtration and the x-ray tube potential affect the amount of filtration needed to achieve a HVL. More inherent filtration would result in a larger HVL for the same kVp. Additionally, more filtration will be needed to achieve a HVL if the maximum photon energy is increased, assuming the inherent filtration is kept constant. If the HVL and kVp are known, the amount of inherent filtration can be determined. If the HVL and amount of inherent filtration are known, the tube operating potential can be determined. Unfortunately, if both the inherent filtration and kVp are unknown, the HVL won't give enough information to determine both.

The OW/Sn ratio was chosen as an independent variable with respect to the HVL. Varying this ratio resulted in the greatest change in the dependent variable – the HVL. Other ratios such as the open window to copper (OW/Cu) ratio and other parameters, such as the OSL reading behind any single filter, were considered but yielded less correlation. The implications of the exponential fitted line from Figure 14 are as follows. The OW/Sn ratio needed to stay within the recommendations of the FDA that the HVL be above a minimum value as specified in Table 1 can be calculated. The equation $HVL = 10.251(OW/Sn)^{-0.7644}$ provides a strong correlation for this purpose as seen in Figure 14.

The purpose of determining different film exposure levels was to provide boundaries as to acceptable film optical densities. Ideally, the film should have an optical density of greater than 0.30 for the regions of interest. In this experiment, the lightest area of interest (the Sn filter position) was to have an optical density of 0.30. The

exposure conditions were varied to meet this criterion. The darkest regions of the film correspondingly had an optical density of just over 3.00. It is not desirable to have an optical density above 3.00 because the human eye cannot readily distinguish contrast levels this dark.

The purpose of digitizing the film was to provide for a way to use software to analyze and quantify several aspects of the film exposure. Once a contrast calibration curve is constructed, as in Figure 20, the film contrast can be analyzed and reported. Because the dose will be reported from the Luxel badge, the radiographic film can be compared to other films that have received similar doses. Significant deviation in optical density compared to other films that have received a similar dose would indicate a possible film processing issue.

The Labview program will be used to perform calculations on the copper grid pattern to determine the grid sharpness. Figure D- 1 shows a picture of the user interface utilized by the Labview program. A very sharp grid could indicate the x-ray tube head is stable and is free of any mechanical drift. A less sharp grid could also indicate poor beam collimation.

This research will be incorporated into a dental survey as follows. First, the cardboard dosimeter holder apparatus and x-ray film will be mailed to the dental facility. The x-ray tube will be positioned at a distance of 5 cm directly in front of the apparatus. The dentist or technician will then make an exposure as they would normally perform on a patient. The film is then to be developed at the dental facility and the film, apparatus,

and the Luxel badge are mailed back to Landauer. Landuaer would follow up by analyzing these results and mailing back a report of the findings.

SUMMARY AND CONCLUSIONS

HVL calculations were performed to establish a means to help further characterize the x-ray beam energy spectrum emerging from a dental x-ray machine. Many older dental x-ray units are still in use today that may not in all ways meet the recommendations set by NRCP and the FDA (NCRP 2003, FDA 1997). The testing proposed in this paper provides a quick and easy way for the x-ray spectrum properties to be surveyed and analyzed. A relationship was derived that relates the OW/Sn ratio to the first HVL. Together, the NCRP and the FDA have given recommendations that limit the acceptable values for the operating tube potential and the HVL (NCRP 2003, FDA 1997). It is important that dental facilities know the performance of their x-ray machines to ensure that limits adopted by the state government are met.

Two aspects of film processing quality were analyzed: exposure settings that result in ideal film optical density and the film sharpness. Film was successfully digitized for analysis through use of software developed by Landauer, Inc. Once digitized, the resultant image will be analyzed to determine the optical densities of the various filter positions. Recommendations based on the degree of over/under exposure can then be made to ensure appropriate exposure settings. A numerical value representing the sharpness of the copper grid was derived which helps determine if any x-ray cone mechanical drift is present or if the beam is not collimated as much as it should be.

Future work to be completed includes a survey of 20 facilities by staff at Landauer using the dosimeter-film apparatus and conventional test tools. After the

completion of this group of facilities, the survey will be sent out to 100 facilities by mail for beta test verification and validation testing.

Future work could also include further testing to extend correlation to cover broader range of HVL's. The range could be expanded to cover HVL's of 0.3 to 7.0 mmAl. Additionally, it would be beneficial to increase sample population used for the derivation of the HVL/dosimeter response relation in order to decrease coefficient of variation.

REFERENCES

Animal Clinic. 2005. Available at http://www.animalcliniccalgary.com/dentistry.htm Accessed 8 August 2005.

Attix FH. Introduction to radiological physics and radiation dosimetry. New York: John Wiley & Sons; 1986

Food and Drug Administration (FDA). Concepts for proposed amendments to the Performance Standard for Diagnostic X-Ray Systems, Center for Devices and Radiological Health: Issued August 1, 1997

Harris, Tom. How X-rays Work. How stuff works. 2002. Available at http://science.howstuffworks.com/x-ray2.htm. Accessed 8 August 2005.

Kaugars GE, Broga DW, Collett WK. Dental radiologic survey of Virginia and Florida. Oral Surgery 60:225-229; 1985

Kircos LT, Staninec M, Chou, L. Effect of developer temperature changes on the sensitometric properties of direct exposure and screen-film imaging systems. Dentomaxillofac. Radiology 18:12-14; 1989

Martin, JE. Physics for radiation protection. New York: John Wiley & Sons; 2000

Napier ID. Reference doses for dental radiography. British Dental Journal 186:392-396; 1999

National Council on Radiation Protection and Measurement (NCRP): Report No. 145 Radiation protection in dentistry, National Council on Radiation: Issued December 31, 2003.

Stavrianou K, Pappous G, Pallikarakis N, Patras. A quality assurance program in dental radiographic units in western Greece. Oral Surg Oral Med Oral Pathol Oral Radiol Endod 1-6; 2005

Svenson B, Eriksson T, Kronstrom M, Palmqvist S. Image quality of intraoral radiographs used by general practitioners in prosthodontic treatment planning. Dentomaxillofac. Radiology 23:46-48; 1994

Texas Department of State Health Services (TDSHS). Texas Administrative Code 289.232: Radiation Control Regulations for Dental Radiation Machines: Issued September 2004. Available at http://www.dshs.state.tx.us/radiation/pdffiles/232fn_04.pdf Accessed 6 September 2005

Yakoumakis EN, Tierris CE, Stefanou EP, Phanourakis IG, Proukakis CC. Image quality assessment and radiation doses in intraoral radiography. Oral Surg Oral Med Oral Pathol Oral Radiol Endod 91:362-368; 2001

APPENDIX A

Table A- 1: Luxel filter raw data: 50 kVp, 1.8 mm Al

Dosimeter	OW Filter	Sn Filter	Cu Filter	Pl Filter
1	362.6	30.7	257.5	305.2
2	357.0	29.0	256.9	312.1
3	349.0	32.2	244.6	301.6
4	326.8	28.2	258.6	312.9
5	403.8	30.5	280.2	340.4
Average	359.9	30.1	259.5	314.4
Std Dev	28.1	1.6	12.9	15.3

Table A- 2: Luxel filter raw data: 60 kVp, 2.4 mm Al

Dosimeter	OW Filter	Sn Filter	Cu Filter	Pl Filter
1	375.0	41.6	286.5	350.1
2	378.6	47.0	308.9	350.7
3	349.3	40.7	272.1	331.8
4	400.2	50.4	287.6	341.5
5	376.2	38.7	273.0	329.6
Average	375.9	43.7	285.6	340.7
Std Dev	18.1	4.8	14.9	9.9

Table A- 3: Luxel filter raw data: 70 kVp, 3 mm Al

Dosimeter	OW Filter	Sn Filter	Cu Filter	Pl Filter
1	343.2	59.2	292.5	319.3
2	365.9	54.9	285.0	341.2
3	370.3	46.7	295.9	309.1
4	360.6	65.2	297.1	342.1
5	375.9	62.3	298.5	323.2
Average	363.2	57.7	293.8	327.0
Std Dev	12.5	7.2	5.4	14.4

Table A- 4: Luxel filter raw data: 80 kVp, 2.8 mm Al

Dosimeter	OW Filter	Sn Filter	Cu Filter	Pl Filter
1	364.0	65.5	299.1	312.7
2	352.1	60.1	279.0	304.9
3	359.0	68.6	266.4	321.3
4	346.2	73.4	286.5	336.5
5	349.0	70.6	270.1	315.2
Average	354.0	67.6	280.2	318.1
Std Dev	7.3	5.1	13.1	11.9

Table A- 5: OW/Sn and HVL correlation

Technique	1st HVL	OW/Sn	$\sigma_{OW/Sn}$
50 kVp, 1.8mmAl	1.516	12.0	1.1
60 kVp, 2.4mmAl	2.003	8.6	1.0
70 kVp, 3mmAl	2.595	6.3	0.8
80 kVp, 2.8mmAl	2.805	5.2	0.4

APPENDIX B

Table B- 1: Calculation of 1st HVL for a beam with 1.8 mm inherent filtration at 50 kVp

Starting Filtration (mm Al)	Potential (kVp)	Current (mA)	
1.8	50	1.5	
Added Filtration (mm Al)	**Air Kerma (mGy)**	**LogKerma**	**Half-Value**
0	1.63	0.21	0.81
1.508	0.82	-0.09	
1.754	0.73	-0.14	
Slope	-0.19	**True HVL (mm Al)**	1.5
Intercept	0.20	**Difference**	-1%
HVL (mm Al)	1.52		

Table B- 2: Calculation of 1st HVL for a beam with 2.4 mm inherent filtration at 60 kVp

Starting Filtration (mm Al)	Potential (kVp)	Current (mA)	
2.4	60	1.2	
Added Filtration (mm Al)	**Air Kerma (mGy)**	**LogKerma**	**Half-Value**
0	1.43	0.16	0.72
2	0.72	-0.15	
2.254	0.67	-0.18	
Slope	-0.12	**True HVL (mm Al)**	2.0
Intercept	0.10	**Difference**	0%
HVL (mm Al)	2.00		

Table B- 3: Calculation of 1st HVL for a beam with 3 mm inherent filtration at 70 kVp

Starting Filtration (mm Al)	Potential (kVp)	Current (mA)	
3	70	1.2	
Added Filtration (mm Al)	**Air Kerma (mGy)**	**LogKerma**	**Half-Value**
0	1.58	0.20	0.79
2	0.90	-0.04	
3	0.72	-0.14	
Slope	-0.10	**True HVL (mm Al)**	2.5
Intercept	0.15	**Difference**	-4%
HVL (mm Al)	2.60		

Table B- 4: Calculation of 1st HVL for a beam with 2.8 mm inherent filtration at 80 kVp

Starting Filtration (mm Al)	Potential (kVp)	Current (mA)	
2.8	80	1	
Added Filtration (mm Al)	**Air Kerma (mGy)**	**LogKerma**	**Half-Value**
0	1.77	0.25	0.89
2	1.04	0.02	
3.508	0.77	-0.11	
Slope	-0.09	**True HVL (mm Al)**	2.9
Intercept	0.19	**Difference**	3%
HVL (mm Al)	2.81		

APPENDIX C

Table C- 1: Current and exposure time needed to achieve normal film exposure at 50 kVp

	O.D. behind filter positions			
	Lightest	Middle	Darkest	
mAs	Sn	Cu	OW	Normal
10	0.24	0.26	0.56	
30	0.26	0.31	1.16	
50	0.28	0.36	1.69	
60	0.29	0.39	1.84	
65	0.30	0.40	1.99	1x
70	0.31	0.43	2.17	
32.5	0.26	0.32	1.24	0.5x
130	0.38	0.59	2.92	2x

Table C- 2: Current and exposure time needed to achieve normal film exposure at 60 kVp

	O.D. behind filter positions			
	Lightest	Middle	Darkest	
mAs	Sn	Cu	OW	Normal
10	0.24	0.29	0.73	
30	0.28	0.41	1.61	
35	0.29	0.43	1.80	
40	0.30	0.47	2.00	1x
45	0.31	0.50	2.17	
50	0.33	0.55	2.33	
20	0.26	0.36	1.19	0.5x
80	0.38	0.71	3.03	2x

Table C- 3: Current and exposure time needed to achieve normal film exposure at 70 kVp

	O.D. behind filter positions			
	Lightest	Middle	Darkest	
mAs	Sn	Cu	OW	Normal
2	0.22	0.24	0.36	
7.5	0.24	0.30	0.74	
20	0.27	0.43	1.57	
24	0.30	0.49	1.90	1x
28	0.30	0.54	2.11	
32	0.31	0.56	2.24	
12	0.27	0.36	1.03	0.5x
48	0.36	0.74	2.67	2x

APPENDIX D

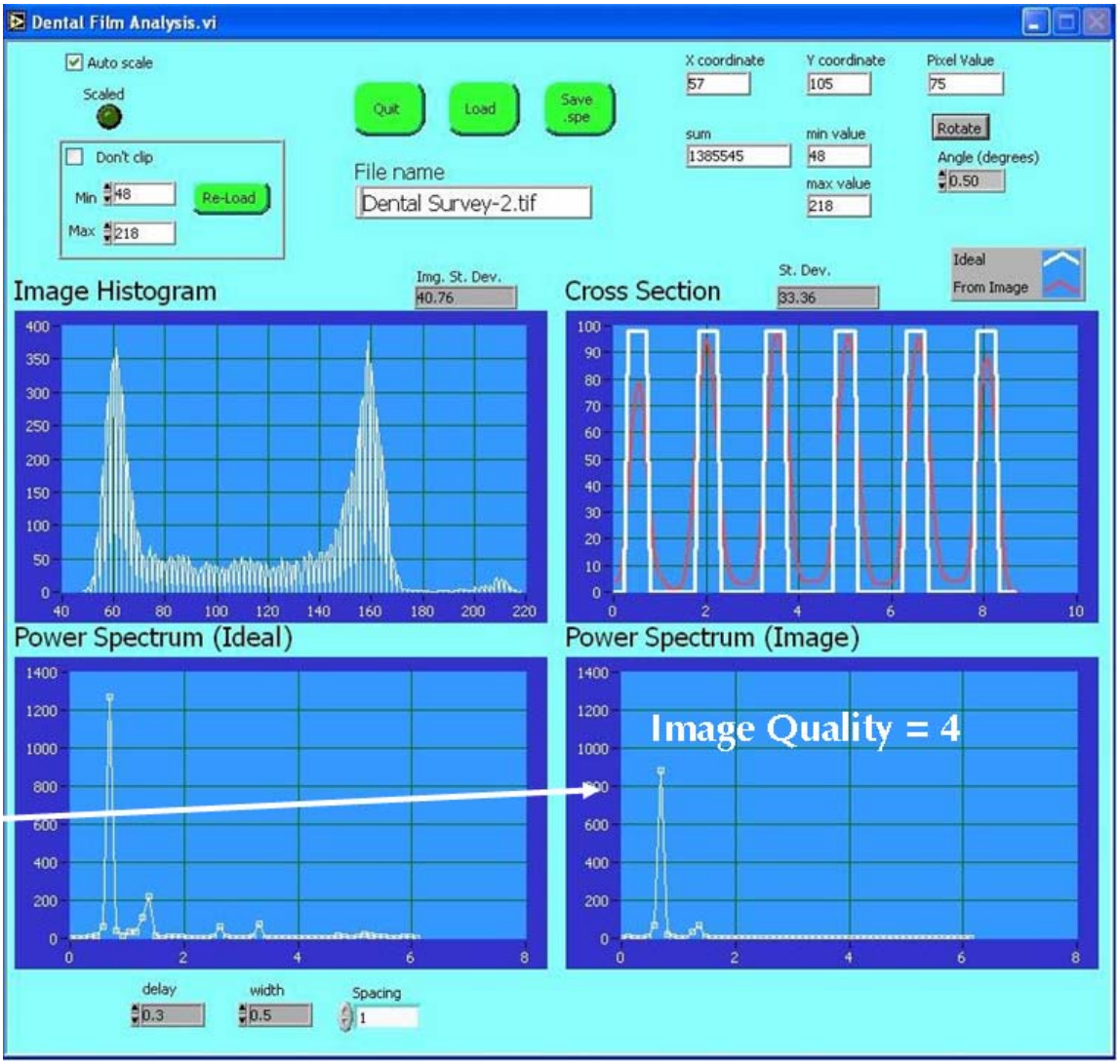

Figure D- 1: Labview main screen

VITA

Name:	Stephen Michael Handley
Address:	601 Lori Dr. Boonville, MO 65233
Email Address:	shandley@tamu.edu
Education:	B.S., Chemical Engineering, University of Missouri-Rolla, 2003 M.S., Health Physics, Texas A&M University, 2005